Supplement of Clim. Past, 12, 2255–2270, 2016
http://www.clim-past.net/12/2255/2016/
doi:10.5194/cp-12-2255-2016-supplement
© Author(s) 2016. CC Attribution 3.0 License.

Climate of the Past
Open Access
EGU

Supplement of

Assessing performance and seasonal bias of pollen-based climate reconstructions in a perfect model world

Kira Rehfeld et al.

Correspondence to: Kira Rehfeld (krehfeld@awi.de) and Mathias Trachsel (mtrachs@umd.edu)

The copyright of individual parts of the supplement might differ from the CC-BY 3.0 licence.

Supplementary Figures and Tables

November 23, 2016

List of Figures

List of Tables

1 Figures

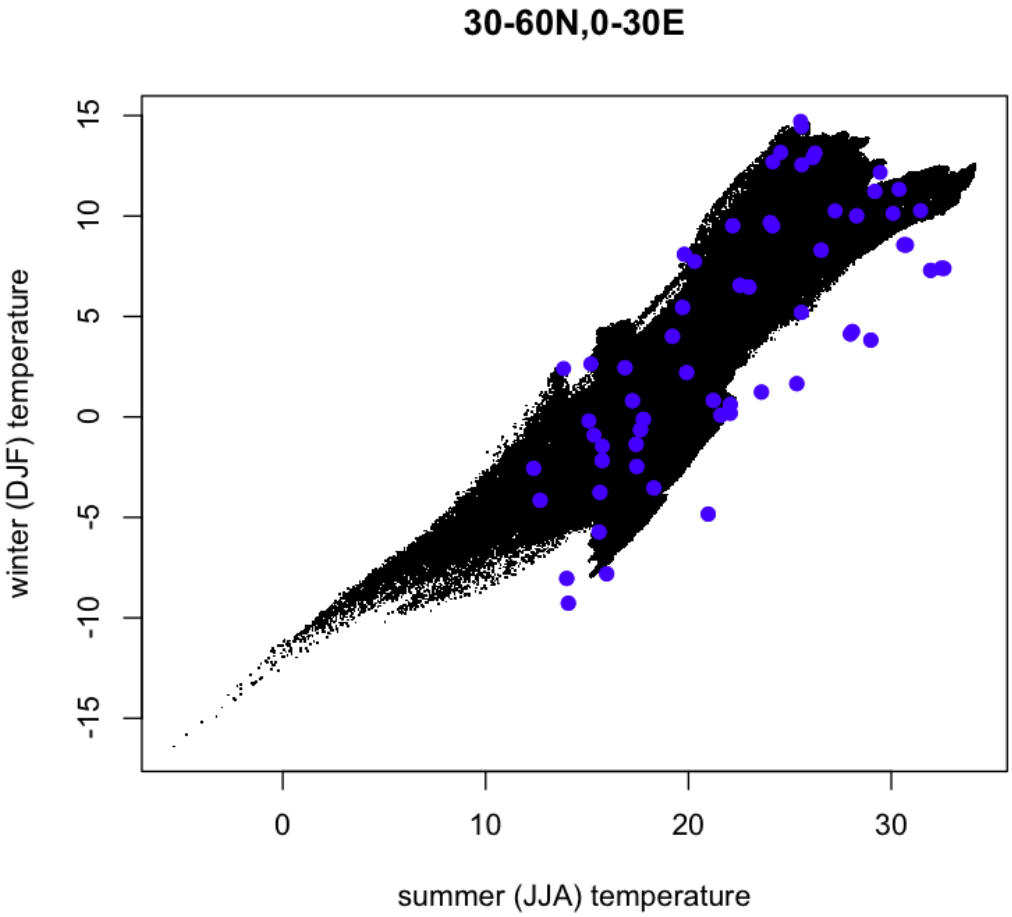

Figure 1: Distribution of European (30-60N, 0-30E) winter and summer temperatures in the 0.5'-resolution temperature field of Hijmans et al. (2005) and in the ECHAM5-MPIOM simulation (Fischer and Jungclaus, 2011) used in this study.The 61 land grid-points from the climate model (blue) cover most of the phase-space spanned by the 13 million grid points of the high resolution field (black), except high-altitude regions represented by the lower-left tail. The model and observed fields further show a similar covariance between the seasons. Thus we do not expect a major influence of the model resolution on our conclusions.

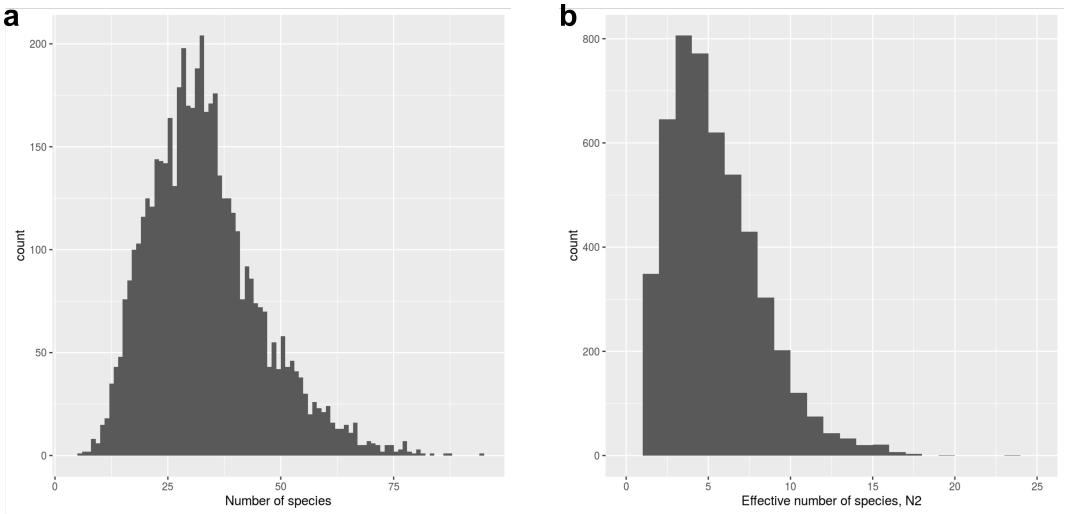

Figure 2: Histogram of the number of species (left) and the effective number of species (as measured by the N_2, (Hill, 1973)) in modern samples in the European Pollen Database (EPD, Davis et al., 2013). The median palynological richness in the 4990 sites in the EPD is 31. However, the median N2 for the fossil data (Fig. 1d in the manuscript) is 2.9, and for the modern calibration data it is 2.7. Therefore, although the number of PFTs is much lower in the model, the diversity and effective number of species is not much lower than in many actual pollen-based climate reconstructions.

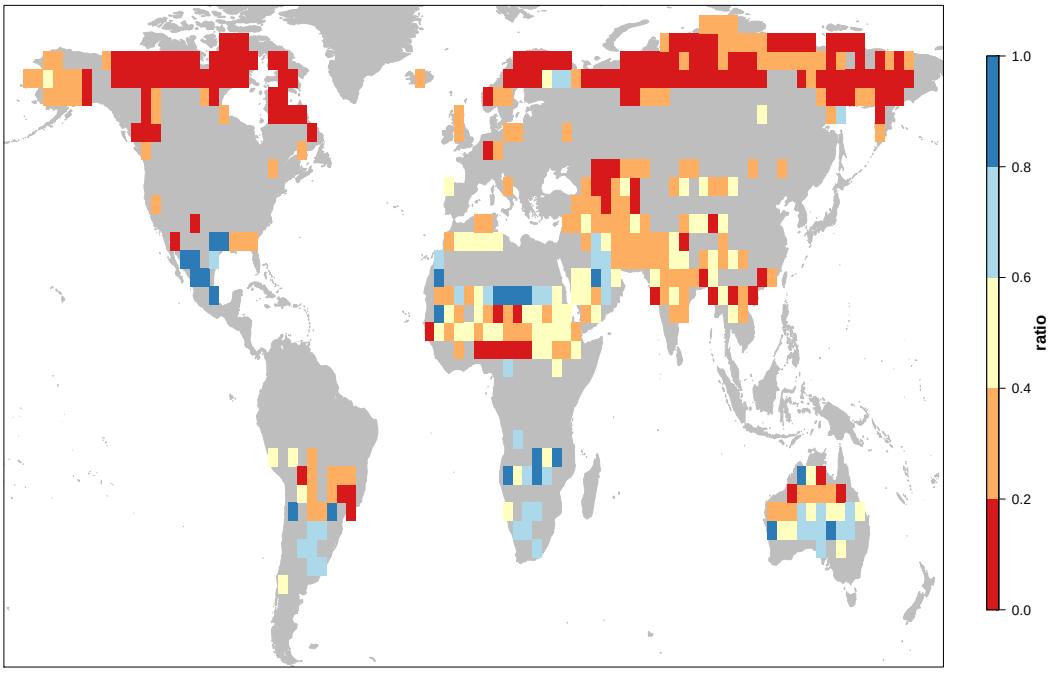

Figure 3: Ratio of the standard deviation of the MTWA climate variable at modern analog sites over the standard deviation within the training set calibration radius. The fact that the ratios are generally smaller than 0.5 illustrates that analog sites are not randomly drawn from the training set.

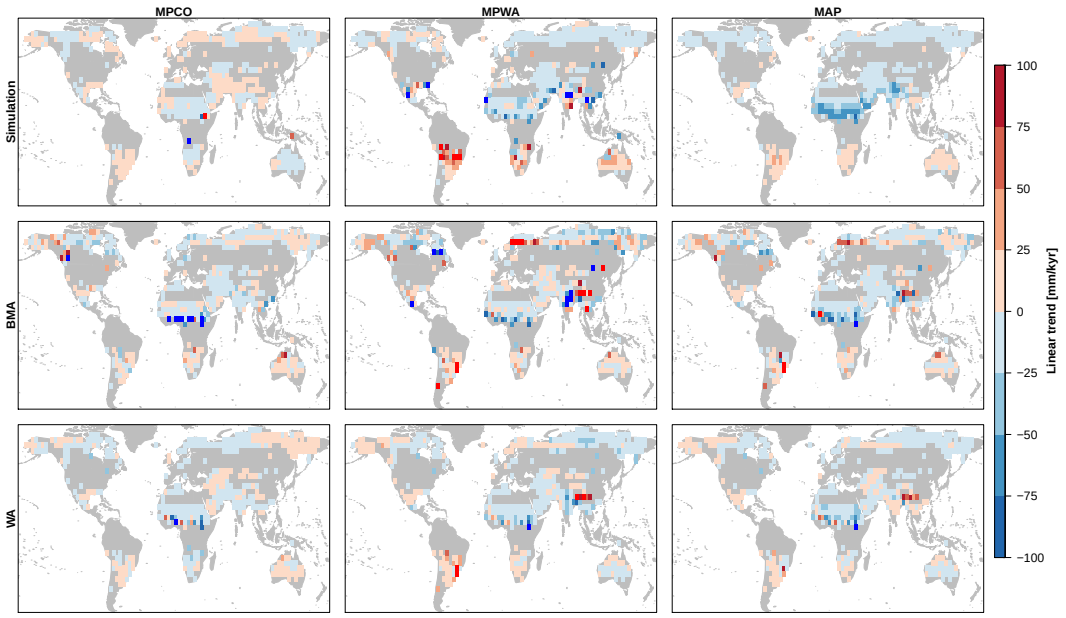

Figure 4: Linear trend in simulated (top) vs. reconstructed precipitation between 6k and present day based on BMA (middle) and WA (bottom).

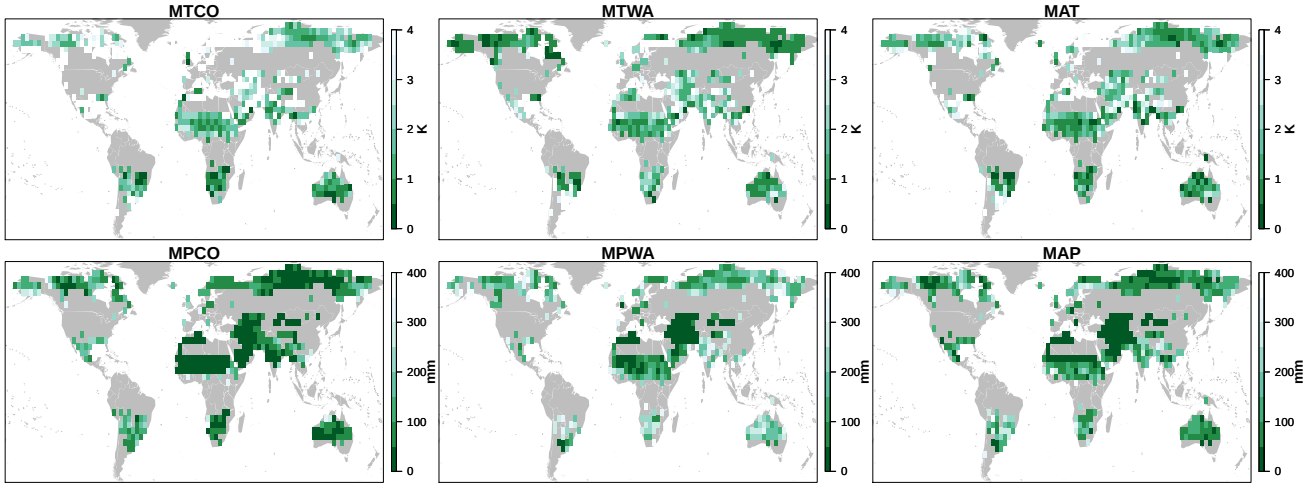

Figure 5: Evaluation of the reconstruction skill. Temporal RMSE of the climate variables reconstructed with the BMA method.

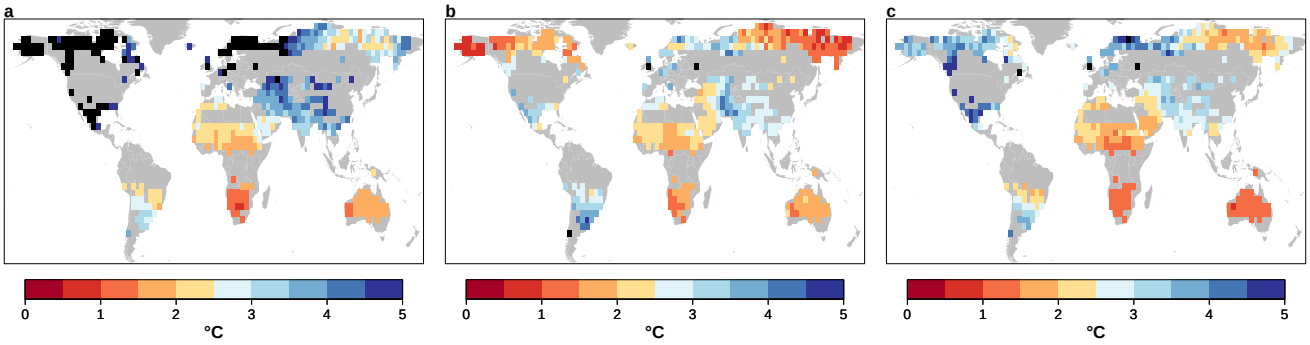

Figure 6: RMSEP for 10-fold-leave-group-out cross-validation of MTCO (a), MTWA (b), MAT (c). Black gridcells indicate a RMSEP larger than 5°C. The RMSEP, particularly for MTCO, is not small. However, it is not much larger than that in real-world large-scale reconstructions (c.p. Fréchette et al., 2008; Mauri et al., 2014).

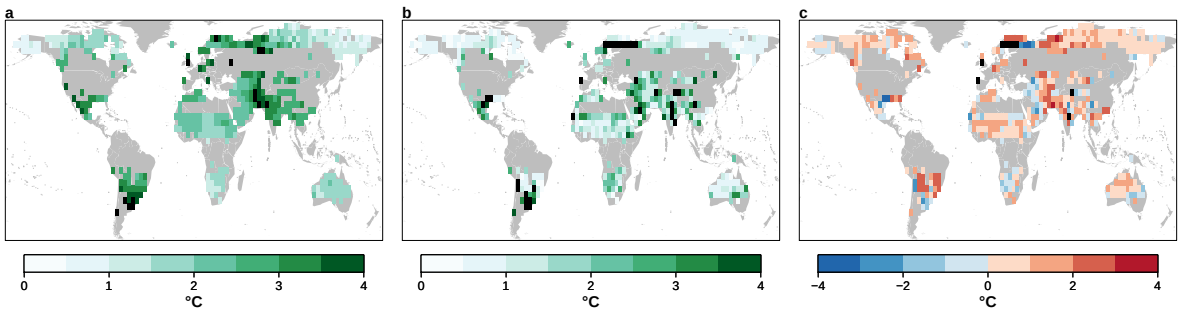

Figure 7: Comparison of spatial calibration (a) and temporal downcore RMSEP (b) and their difference (c) for a BMA based reconstruction of MTWA.

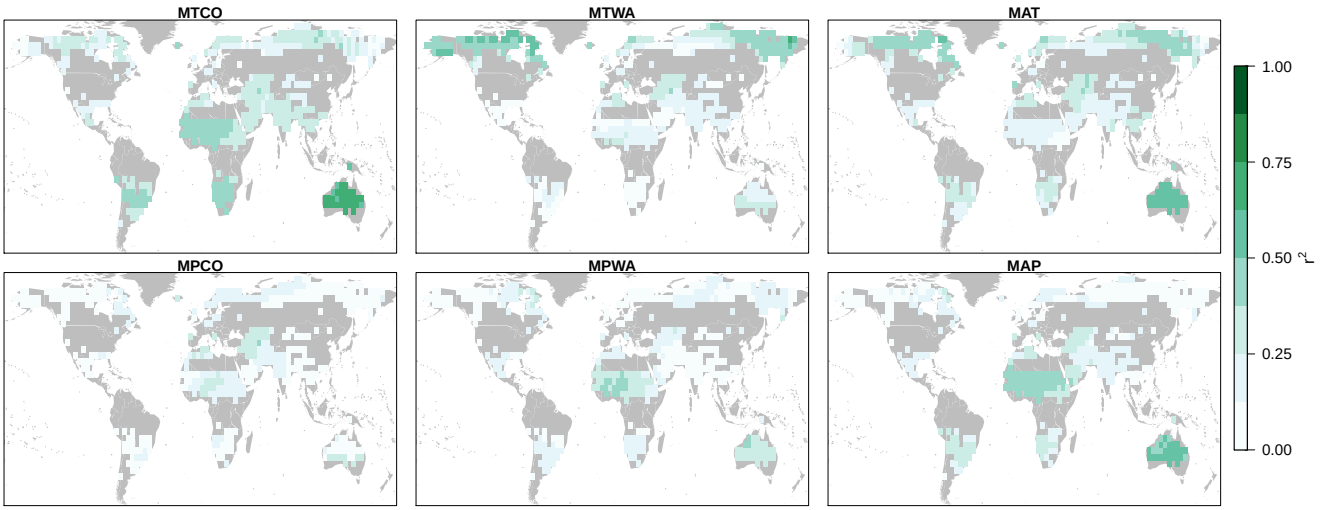

Figure 8: Modern spatial vegetation variance, based on CCA, explained by climate variables across modern space. High values indicate that climate variable and vegetation changes within the 2500km radius are correlated. Fields summarized in Fig. 6a and SF 11a.

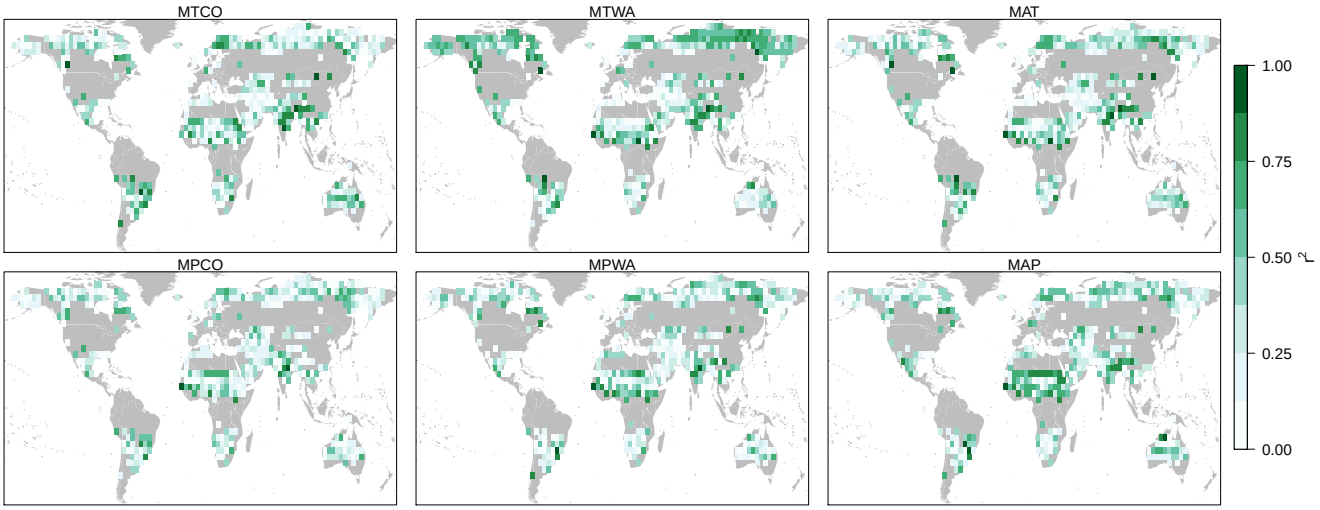

Figure 9: Fossil vegetation variance explained by the reconstructed climate variables in RDA. High values indicate that the reconstructed climate variability is correlated in time with vegetation variability. Fields summarized in Fig. 6b and SF 11b.

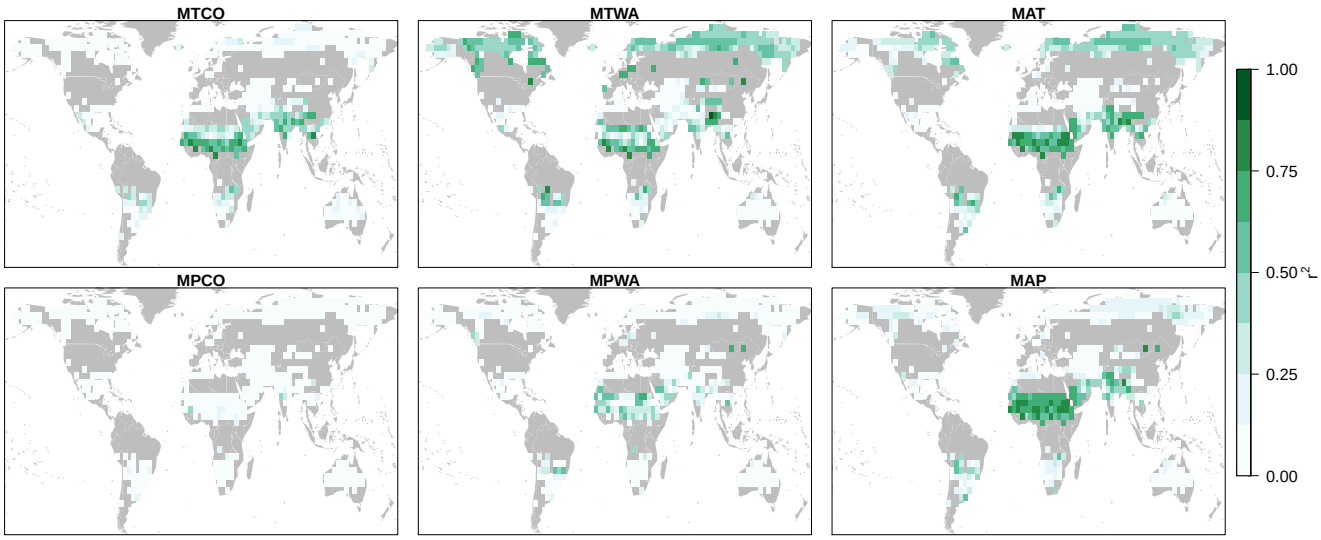

Figure 10: Fossil vegetation variance explained by simulated climate variables in RDA. High values indicate, whether a climate variable was driving vegetation changes - or that its temporal changes were correlated to another such variable. Fields summarized in Fig. 6c and SF 11c.

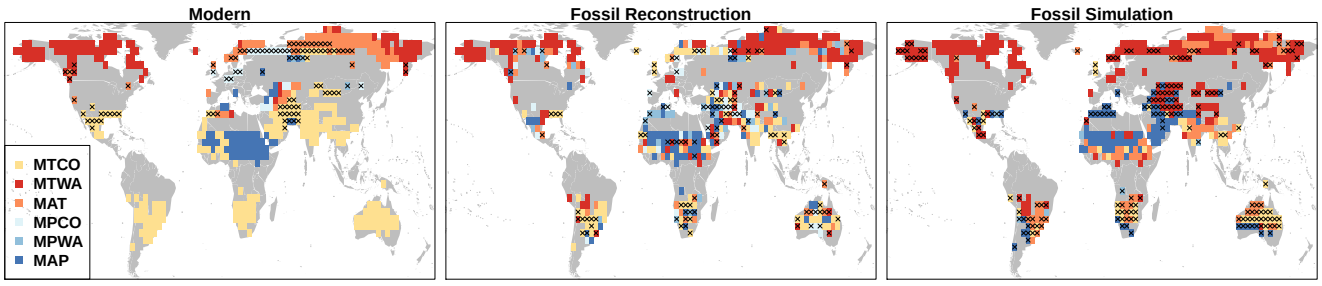

Figure 11: Climate variables with the highest λ_1/λ_2 ratio based on CCA in modern vegetation (a), on RDA between reconstructed climate and fossil vegetation (b) and simulated climate and fossil vegetation (c). Black circles mark grid cells where the most prominent gradient ratio is still below 1.

2 Tables

Table 1: Bioclimatic temperature limits for the PFTs in the coupled model simulation. Growing degree days (GDD5) are given as the temperature sum of days which exceed 5°C. Adapted from Dallmeyer et al. (2011).

PFT	**landcover/phenology**	$\mathbf{MTCO_{min}}$ [°C]	$\mathbf{MTCO_{max}}$ [°C]	$\mathbf{MTWA_{max}}$ [°C]	**GDD5** [°C]
teT	tropical evergreen trees	15.5	–	–	0
tdT	tropical deciduous trees	15.5	–	–	0
eteT	extratropical evergreen trees	-32.5	18.5	–	350
etdT	extratropical deciduous trees	–	18.5	–	350
rS	raingreen shrubs	0	–	–	900
cS	cold shrubs	–	-2	18	300
C3	C3 grass	–	15	–	0
C4	C4 grass	10	–	–	0

References

Davis, B. A. S., Zanon, M., Collins, P., Mauri, A., Bakker, J., Barboni, D., Barthelmes, A., Beaudouin, C., Bjune, A. E., Bozilova, E., Bradshaw, R. H. W., Brayshay, B. A., Brewer, S., Brugiapaglia, E., Bunting, J., Connor, S. E., de Beaulieu, J. L., Edwards, K., Ejarque, A., Fall, P., Florenzano, A., Fyfe, R., Galop, D., Giardini, M., Giesecke, T., Grant, M. J., Guiot, J., Jahns, S., Jankovská, V., Juggins, S., Kahrmann, M., Karpińska-Kołaczek, M., Koaczek, P., Kühl, N., Kunes, P., Lapteva, E. G., Leroy, S. A. G., Leydet, M., López Sáez, J. A., Masi, A., Matthias, I., Mazier, F., Meltsov, V., Mercuri, A. M., Miras, Y., Mitchell, F. J. G., Morris, J. L., Naughton, F., Nielsen, A. B., Novenko, E., Odgaard, B., Ortu, E., Overballe-Petersen, M. V., Pardoe, H. S., Peglar, S. M., Pidek, I. A., Sadori, L., Seppä, H., Severova, E., Shaw, H., Świeta-Musznicka, J., Theuerkauf, M., Tonkov, S., Veski, S., van der Knaap, W. O., van Leeuwen, J. F. N., Woodbridge, J., Zimny, M., and Kaplan, J. O.: The European Modern Pollen Database (EMPD) project, Veg. Hist. Archaeobot., 22, 521–530, doi:10.1007/s00334-012-0388-5, 2013.

Fischer, N. and Jungclaus, J. H.: Evolution of the seasonal temperature cycle in a transient Holocene simulation: orbital forcing and sea-ice, Clim. Past, 7, 1139–1148, doi:10.5194/cp-7-1139-2011, 2011.

Fréchette, B., de Vernal, A., Guiot, J., Wolfe, A. P., Miller, G. H., Fredskild, B., Kerwin, M. W., and Richard, P. J. H.: Methodological basis for quantitative reconstruction of air temperature and sunshine from pollen assemblages in Arctic Canada and Greenland, Quat. Sci. Rev., 27, 1197–1216, doi:10.1016/j.quascirev.2008.02.016, 2008.

Hijmans, R. J., Cameron, S. E., Parra, J. L., Jones, P. G., and Jarvis, A.: Very high resolution interpolated climate surfaces for global land areas, Int. J. Climatol., 25, 1965–1978, doi:10.1002/joc.1276, 2005.

Hill, M. O.: Diversity and evenness: a unifying notation and its consequences, Ecology, 54, 427–432, doi:10.2307/1934352, 1973.

Mauri, A., Davis, B. A. S., Collins, P. M., and Kaplan, J. O.: The influence of atmospheric circulation on the mid-Holocene climate of Europe: a data–model comparison, Clim. Past, 10, 1925–1938, doi:10.5194/cp-10-1925-2014, 2014.